

STIFFENING EFFECT ON END BEARING GRANULAR PILES

M. R. Madhav¹, Jitendra Kumar Sharma² and Vaibhaw Garg³

¹Civil Engineering Dept., Jawaharlal Nehru Technological University, Hyderabad 500072, India

^{2,3}Civil Engineering Dept., Rajasthan Technical University, University Department, Kota-324010, India

¹E-mail: madhavmr@gmail.com

²E-mail: jksharma@rtu.ac.in

³E-mail: vgarg@rtu.ac.in

ABSTRACT: The performance of ground improvement using granular piles (GP) is limited by its low strength and stiffness. If GPs are partially strengthened and stiffened near the ground surface, their overall performance gets enhanced several fold. Stiffening of GP can be achieved by replacing partially the upper portion of GPs with material having higher strength and deformation modulus, e.g. by geo-synthetic encased columns, SDCM (stiffened deep cement mixing), etc. Analyses of a single and group of two partially stiffened end bearing GPs is presented in terms of top settlement influence factor, settlement interaction factor for two-pile group, settlement reduction factor, percentage load transferred to the base, variation of normalized shear stress distribution along the length of the pile. Settlement influence factor decreases while the percentage load transferred to the base of increases with increase in the relative stiffness factor and the relative length of stiffening from top of the partially stiffened GP, both for single as well as for two pile group.

KEYWORDS: Relative stiffness of bearing stratum, Relative stiffness of granular pile, Settlement influence factor, Settlement interaction factor, and Settlement reduction factor

1. INTRODUCTION

In this paper analyses of axially loaded single and group of two end bearing granular piles, partially stiffened each based on the elastic continuum approach are presented. Soil displacement matrix is generated by integrating, Mindlin's (1936) equations. The mirror image technique of solution developed by Mattes and Poulos (1969) for end-bearing piles is used for obtaining the solution. Pile displacement matrix is developed for the evaluation of the vertical displacement of the pile incorporating the relative stiffness factor and relative length of stiffening from top of GP.

The following assumptions are made: (i) Soil is homogeneous, isotropic and linearly elastic; (ii) The base of stone column/granular pile is smooth across which the load is distributed uniformly (Madhav et al. 2006); (iii) Effect due to the installation of granular piles and (iv) Slip or yield at the pile – soil interface not considered.

2. LITERATURE REVIEW

Poulos and Mattes (1969, 1971) were pioneers in presenting the settlement analysis of a group of compressible piles. Sharma et al. (2004) report increase in the load-carrying capacity of geogrid-reinforced GP with an increase in the number of geogrids and a decrease in the spacing between them. The carrying capacity of encapsulated sand columns was found to increase due to increases in strength and length of the geo-fabric (Ayadat and Hanna 2005). Madhav et al. (2006) analyse settlement of a granular pile considering non-homogeneities in the deformation moduli and strength of in situ ground and of granular pile material. Murugesan and Rajagopal (2006) using FEM studied the effect of encasing stone columns with geosynthetic material for improvement in the load carrying capacity of the stone columns. Black et al. (2007) experimentally investigated the performance of a stone column by jacketing the column with a tubular wire mesh. Jamsawang et al. (2008) studied the performance of a stiffened deep mixed pile. Murugesan and Rajagopal (2010) investigated the performance of encased stone columns through 1-g laboratory tests. Lo et al. (2010) presented the results of a time dependent coupled FE analysis that utilized the unit cell concept to study the bearing and settlement responses of stone columns reinforced with geosynthetic encasements under embankment-type loading. Pulko et al. (2011) proposed an analytical model for designing encased and ordinary stone columns in soft clays. Shahu and Reddy (2011) conducted fully drained 1-g model tests on unit cell of granular pile reinforced soft

soil. Castro and Sagaseta (2011) presented an analytical model for studying the improvement brought by encased stone columns on settlement and consolidation time of soft clays. Niroumand et al. (2011) conducted experimental work on soil improvement by stone columns reinforced with horizontal meshes. Marto et al. (2013), Zhang and Zhao (2015) and Hong et al. (2016) studied analytically as well as experimentally the effects of encasement stiffness and strength on the response of individual geo-textile encased granular columns embedded in soft soil. Garg and Sharma (2018) analyze analytically settlement of single and group of two partially stiffened floating granular piles.

3. PROBLEM DEFINITION AND ANALYSIS

A single GP bearing on a relatively stiff layer is of length 'L', diameter, 'd'=(2a) and subjected to an axial load 'P' (Figures 1(a)-(b)). GP is stiffened partially over a length, L_s to overcome the limitations of bulging near the top. Figure 2(a) depicts group of two end bearing partially stiffened (over length, L_s) GPs each of length 'L', diameter 'd'=(2a), center to center spacing of 's' and each pile being subjected to axial load 'P'. In situ soil has deformation modulus, 'E_s' and Poisson's ratio, 'ν_s'. The deformation moduli of the granular pile in the un-stiffened and stiffened portions are 'E_{gp}' and 'E_{gpst}' respectively. The relative stiffness of GP is defined as $K_{gp}=E_{gp}/E_s$, i.e., the ratio of deformation modulus of granular pile to that of the in situ soil. The relative stiffness of the bearing stratum is defined as $K_b=E_b/E_s$, where E_b is the modulus of deformation of the bearing stratum. Parameters, 'χ' (=E_{gpst}/E_{gp}) and 'η' (=L_s/L) define the relative stiffness factor and relative length of stiffening from top of GP respectively. Elastic continuum approach with mirror image technique (Figure 2(b)) following Poulos and Davis (1980) is employed for the analysis of end-bearing compressible pile.

3.1 Soil Displacements

GP is discretised into 'n' cylindrical elements of length, $\Delta L=L/n$. Shear stress, τ, acts along the shaft elements and a uniform pressure, p_b, acts on the base. The discretisation and the integration scheme follow the method proposed by Poulos and Davis (1980) and are based on Mindlin (1936). Soil displacements of the nodes on the periphery of each element of GP and at the centre of base are evaluated and summed over all the elements for the influences of all

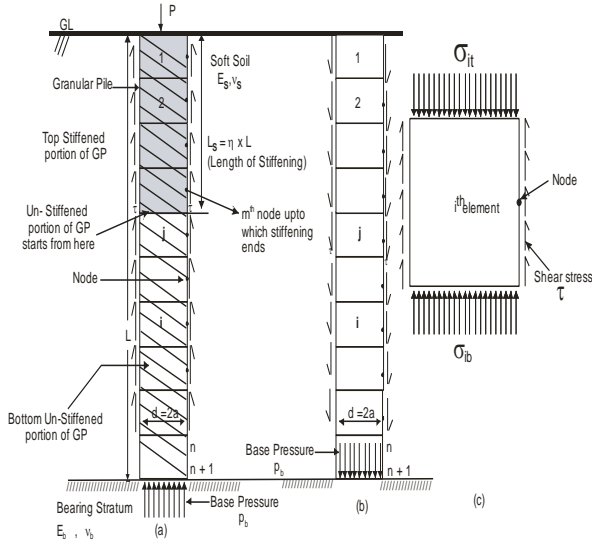


Figure 1 (a) Force and stresses on a single end bearing, partially stiffened GP, (b) Stresses in the soil due to GP and (c) Stresses on any i^{th} element of the GP (Courtesy: Sharma (1999))

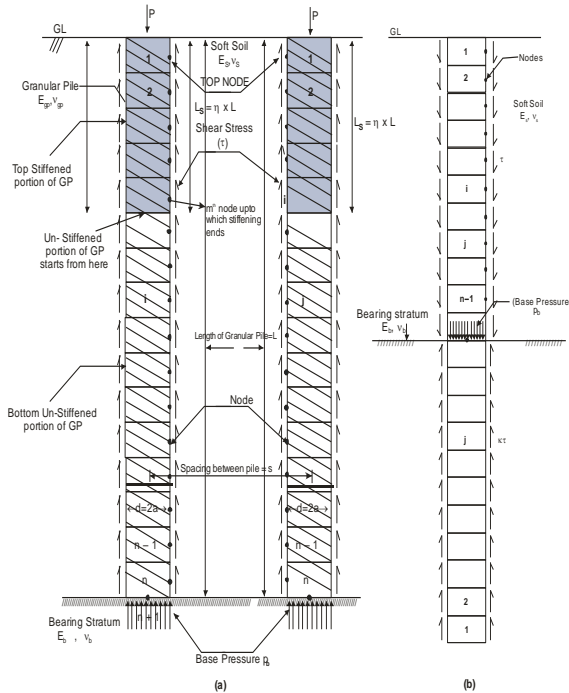


Figure 2(a) Definition sketch for two end bearing partially stiffened GPs (b) Mirror image technique for granular pile resting on bearing stratum (Mattes and Poulos 1969)

the elemental shear stresses. The set of soil displacements equations for an end bearing granular pile as per Mattes and Poulos (1969) are

$$\left\{ \rho^s \right\} = \left\{ \frac{S^s}{d} \right\} = \left[\left[I^{sp} \right] - \kappa \left[I^{spim} \right] \right] \left\{ \frac{\tau}{E_s} \right\} \quad (1)$$

where $\{S^s\}$ and $\{\rho^s\}$ are soil displacement and normalized soil displacement vectors respectively of size ' n '. $\{\tau/E_s\}$ is a column vector of size ' n ' for the normalized shear stresses. $[I^{sp}]$ is a square matrix of soil displacement influence coefficients of size ' n '. $[I^{spim}]$ is a square matrix of soil displacement influence coefficients due to

shear stresses on image elements of size ' n '. The influence of the shear stresses on mirror image elements is taken as κ times the influence of shear stresses on the real elements in the negative direction, where κ is a non-dimensional parameter that accounts for the compressibility of the base that lies between 0 (floating GP) and 1 (GP resting on a rigid stratum, $E_b/E_s \rightarrow \infty$) respectively.

3.2 Pile Displacements

Settlement of the base of a GP resting on a bearing stratum of finite compressibility is obtained (following Mattes and Poulos, 1969) from Boussinesq's equation for the vertical displacement of a rigid circular disc on a semi-infinite mass as

$$\rho_b^p = \frac{S_b^p}{d} = \frac{p_b (1 - \nu_b^2) \pi / 4}{E_b} \quad (2)$$

where S_b^p and ρ_b^p are respectively the settlement of the GP at the base and normalized settlement of the GP at the base.

The base pressure, ' p_b ', is expressed in terms of shear stresses, ' τ_j ', as

$$p_b = \frac{P}{\pi d^2 / 4} - \frac{4(L/d)}{n} \sum_{j=1}^{j=n} \tau_j \quad (3)$$

The settlement of the base in terms of the applied load and mobilized shear stresses (using Eqs. (2)- (3)) is

$$\rho_b = \left[\frac{P}{E_s \pi d^2 / 4} - \frac{4(L/d)}{n} \sum_{j=1}^{j=n} \frac{\tau_j}{E_s} \right] \times \frac{\pi (1 - \nu_b^2)}{4(E_b/E_s)} \quad (4)$$

The axial stresses on the top and bottom faces of the element ' i ', (Figure 1(c)) are

$$\begin{aligned} \sigma_{it} &= p_b + \sum_{j=i}^{j=n} \frac{4(L/d) \tau_j}{n} \\ \sigma_{ib} &= p_b + \sum_{j=(i+1)}^{j=n} \frac{4(L/d) \tau_j}{n} \end{aligned} \quad (5)$$

The average axial stress on the element, ' i ', is equal to

$$\sigma_i = \frac{\sigma_{it} + \sigma_{ib}}{2} = p_b + \sum_{j=(i+1)}^{j=n} \frac{4(L/d) \tau_j}{n} + \frac{2(L/d) \tau_i}{n} \quad (6)$$

Settlement of n^{th} element is estimated as the sum of the settlement of the base plus the settlement of the n^{th} element due to the axial stress, ' ρ_n^p ', acting on it as

$$\rho_n^p = \rho_b^p + \frac{\sigma_n (\Delta z / 2d)}{E_{gp}} \quad (7)$$

where ' σ_n/E_{gp} ', is axial strain of the n^{th} element and Δz element length. The settlement, ρ_i^p , of any element ' i ', of GP is,

$$\rho_i^p = \rho_b^p + \sum_{j=n}^{j=i-1} \frac{\sigma_j}{E_{gpj}} (\Delta z/d) + \frac{\sigma_i}{E_{gpi}} (\Delta z/2d) \quad (8)$$

where ‘ σ_i ’ is the normal stress on element, ‘ i ’. Due consideration is given to maintain the compatibility of displacements at the interface of stiffened and un-stiffened portions of GP. Stiffening is carried out till the bottom of the m^{th} element from the top of the GP as shown in Figures 1(a) and 2(a). The displacement at the bottom of the m^{th} element or top of $(m+1)^{th}$ element i.e., interface of stiffened and un-stiffened portion of GP is

$$\rho_{interface}^p = \rho_b^p + \sum_{j=n}^{j=m+1} \frac{\sigma_j}{E_{gp}} (\Delta z/d) \quad (9)$$

where ‘ E_{gp} ’, is the deformation modulus of the un-stiffened GP.

The displacement of the bottom of the m^{th} element of stiffened portion is taken as the displacement of the top of the $(m+1)^{th}$ element of un-stiffened portion of GP in order to satisfy the compatibility of displacements at the interface between two. The displacement of the node at the center of m^{th} element is

$$\rho_{i=m}^p = \rho_b^p + \sum_{j=n}^{j=m+1} \frac{\sigma_j}{E_{gp}} (\Delta z/d) + \frac{\sigma_i}{E_{gpst}} (\Delta z/2d) \quad (10)$$

where ‘ E_{gp} ’, and ‘ E_{gpst} ’ are the deformation moduli of un-stiffened and the stiffened lengths of the GP. The above set of displacement equations are expressed in matrix form as

$$\{\rho^p\} = \rho_b \{1\} + [\Delta_1] \left\{ \frac{\sigma}{E_s} \right\} \quad (11)$$

where {1} – a unit column vector and $[\Delta_1]$ - a matrix of size $(n \times n)$ is defined below

$$[\Delta_1] = \frac{(L/d)}{nK_{gp}} \begin{bmatrix} 0.5 & 1 & 1 & 1 & - & - & - & - & - & 1 \\ \chi & \chi & \chi & & & & & & & \\ 0 & 0.5 & 1 & 1 & - & - & - & - & - & 1 \\ & \chi & \chi & & & & & & & \\ 0 & 0 & 0.5 & 1 & - & - & - & - & - & 1 \\ \cdot & \cdot \\ 0 & 0 & 0 & 0.5 & - & - & - & - & - & 1 \\ \cdot & \cdot \\ 0.5 & 1 & 1 & 1 & 1 & 1 & 1 & 1 & 1 & 1 \\ 0 & 0.5 & 1 & 1 & 1 & 1 & 1 & 1 & 1 & 1 \\ \cdot & \cdot \\ 0 & 0 & 0 & 0 & 0 & 0 & 0 & 0 & 0 & 0.5 \end{bmatrix} \quad (12)$$

$[\Delta_1]$ is an upper triangular matrix as per Eqs. (8) - (10) and incorporates the parameters i.e. relative stiffness factor, χ and relative length, η , of stiffening from top of GP, for the stiffened granular pile.

Combining Eqs. (4) - (11) one gets

$$\{\rho^p\} = \frac{P(1-v_b^2)}{(E_b/E_s)d^2 E_s} \{1\} - \frac{\pi(L/d)(1-v_b^2)}{n(E_b/E_s)} [1] \left\{ \frac{\tau}{E_s} \right\} + [\Delta_1] \left\{ \frac{\sigma}{E_s} \right\} \quad (13)$$

where {1} and [1] are respectively column vector and square matrix of size ‘ n ’. The shaft shear stresses and the axial stresses of each element are related (based on equilibrium relationship) as

$$\sigma_i = \frac{P}{(\pi d^2/4)} - \sum_{j=1}^{j=i-1} \frac{4\tau_j L}{nd} - \frac{2\tau_i L}{nd} \quad (14)$$

The above equation in matrix form is

$$\left\{ \frac{\sigma}{E_s} \right\} = \frac{P}{(\pi d^2/4)E_s} - \frac{4(L/d)}{n} [\Delta_2] \left\{ \frac{\tau}{E_s} \right\} \quad (15)$$

where $[\Delta_2]$ is lower triangular matrix of size ‘ n ’ in which the diagonal and off diagonal terms are 0.5 and 1.0 respectively. Using the relationship between axial stresses and shaft shear stresses (Eq. (15)) the final form of displacement equations for elements $i = 1$ to n in terms of shaft shear stresses (Eq. (13)) are

$$\{\rho^p\} = \{Y\} + [\Delta] \left\{ \frac{\tau}{E_s} \right\} \quad (16)$$

Where

$$\{Y\} = \frac{P(1-v_b^2)}{(E_b/E_s)d^2 E_s} \{1\} + \frac{P}{(\pi d^2/4)E_s} [\Delta_1] \{1\} \quad (17)$$

$$[\Delta] = -\frac{4(L/d)}{n} [\Delta_1] [\Delta_2] - \frac{\pi(L/d)(1-v_b^2)}{n(E_b/E_s)} [1]$$

4. COMPATIBILITY OF SOIL AND PILE DISPLACEMENTS

Satisfying the compatibility of vertical displacements of the granular pile and the soil, solutions are obtained in terms of interface shear stresses and base pressure. For single granular pile resting on stiff bearing stratum, (Eqs. (1) - (16)), the interface shear stresses are

$$\left\{ \frac{\tau}{E_s} \right\} = \left[\left[I^{sp} \right] - \kappa \left[I^{spim} \right] - [\Delta] \right]^{-1} \{Y\} \quad (18)$$

For estimation of κ , an iterative technique suggested by Mattes and Poulos (1969) is used. With an initial chosen value of κ , Eqs. (18) - (3) are solved to estimate the ‘ n ’ unknown shear stresses, ‘ τ ’, and the base pressure, ‘ p_b ’. Having obtained the solution for chosen value of κ , a closer estimate of the correct value of κ is obtained by considering the compatibility of displacements of soil and the bearing stratum at the pile tip. The soil displacement at the pile tip, ρ_b^s is

$$\rho_b^s = \frac{S_b^s}{d} = \left\{ I_j^{sb} - \kappa I_j^{sbim} \right\} \left\{ \frac{\tau}{E_s} \right\} = \frac{\sum_{j=1}^{j=n} (I_j^{sb} - \kappa I_j^{sbim}) \tau_j}{E_s} \quad (19)$$

Where $I_j^{sb}=I_j^{sbim}$ are displacement influence coefficients for the tip due to shear stresses on real and imaginary elements 'j', respectively. Due to symmetry $I_j^{sb}=I_j^{sbim}$. Equating the soil displacement at the pile tip to the displacement of the base due to base stress, p_b (Eq. (2)) the new value of the parameter, κ , is obtained as

$$\kappa = 1 - \frac{\pi(1 - \nu_b^2) p_b}{4(E_b/E_s) \sum_{j=1}^n \tau_j I_j^{sb}} \quad (20)$$

Eq. (18) is solved iteratively using the new value of κ , and the process repeated until the required convergence (the percentage difference between the new and the previous values of κ is less than 0.01%) is obtained.

The same analysis as described above was developed for a group of two end bearing piles. For a group of two granular pile resting on a stiff bearing stratum

$$\left\{ \rho^s \right\} = \left\{ \frac{S^s}{d} \right\} = \left[\begin{array}{c} [1I^{sp}] + [2I^{sp}] - \kappa [1I^{spim}] \\ \kappa [2I^{spim}] \end{array} \right] \left\{ \frac{\tau}{E_s} \right\} \quad (21)$$

where $\{S^s\}$ and $\{\rho^s\}$, are soil displacement and normalized soil displacement vectors of size 'n' respectively; $\{\tau\}$ a column vector of size 'n' for GP-soil interface shear stresses. Similarly, $[[1I^{sp}]+[2I^{sp}]-\kappa[1I^{spim}]]$ is a square matrix of soil displacement influence coefficients of size 'n' for end-bearing granular piles. $[1I^{sp}]$ and $[2I^{sp}]$, are matrices of displacement influence coefficients due to shear stresses on own and adjacent GPs respectively while $[1I^{spim}]$ and $[2I^{spim}]$ are soil displacement influence coefficients due to, respectively, shear stresses on imaginary elements of own and adjacent GP. The values of $[1I^{sp}]$, $[2I^{sp}]$, $[1I^{spim}]$ and $[2I^{spim}]$ are obtained by integration of Mindlin's equation for vertical displacement in semi-infinite mass. The method described by Poulos and Mattes (1971) for interaction of one pile with the other in group of two piles is used.

For a two granular pile group resting on stiff bearing stratum (Eqs. (16) - (21)) for the interface shear stresses get modified as

$$\left\{ \frac{\tau}{E_s} \right\} = \left[\begin{array}{c} [1I^{sp}] + [2I^{sp}] - \kappa [1I^{spim}] \\ -\kappa [2I^{spim}] \end{array} \right]^{-1} \left\{ \frac{\Delta}{E_s} \right\} \quad (22)$$

For the estimation of κ , an iterative technique suggested by Mattes and Poulos (1969) and described above is used. From the equilibrium equation, the base pressure, ' p_b ', can be obtained as

$$p_b = \frac{P}{\pi d^2/4} - \frac{4(L/d)}{n} \sum_{j=1}^n \tau_j \quad (23)$$

The soil displacement at the pile tip is

$$\rho_b^s = \frac{S_b^s}{d} = \left\{ \left\{ [1I_j^{sb}] \right\} + \left\{ [2I_j^{sb}] \right\} - \kappa \left\{ [1I_j^{sbim}] \right\} - \kappa \left\{ [2I_j^{sbim}] \right\} \right\} \left\{ \frac{\tau}{E_s} \right\} \\ = \frac{\sum_{j=1}^n \left([1I_j^{sb}] + [2I_j^{sb}] - \kappa [1I_j^{sbim}] - \kappa [2I_j^{sbim}] \right) \tau_j}{E_s} \quad (24)$$

where, $1I_j^{sb}$, $1I_j^{sbim}$ and $2I_j^{sb}$, $2I_j^{sbim}$ are the displacement influence coefficients for the tip due to shear stresses on real and imaginary elements 'j' of own and adjacent GP respectively. However due to symmetry, $1I_j^{sb} = 1I_j^{sbim}$ and $2I_j^{sb} = 2I_j^{sbim}$. Equating the soil displacement at the pile tip to the displacement of the base due to base stress, ' p_b ' (Eq. (2)) the new value of non-dimensional parameter, κ , is obtained as

$$\kappa = 1 - \frac{\pi(1 - \nu_b^2) p_b}{4(E_b/E_s) \sum_{j=1}^n \tau_j \left([1I_j^{sb}] + [2I_j^{sb}] \right)} \quad (25)$$

Eq. (25) is solved iteratively using the new value of κ , and the process repeated until the required convergence (as mentioned above) is obtained.

Settlement influence factor for any depth, I_{spd} , for a single un-stiffened & stiffened GP and for a GP in a group of two un-stiffened & partially stiffened GP is defined as,

$$S_{\text{any depth}} = \frac{P}{\frac{\pi}{4} E_s d} I_{spd} \quad (26)$$

where 'P', is load on single or on each GP in group of two, $S_{\text{any depth}}$ is the settlement at any depth.

The top settlement influence factor, I_{sp} , of un-stiffened & stiffened single and group of two un-stiffened & partially stiffened GP is

$$S_{TOP} = \frac{P}{\frac{\pi}{4} E_s d} I_{sp} \quad (27)$$

where I_{sp} , is the settlement influence factor corresponding to top displacement and S_{TOP} is the settlement at top of GP. The overall response of the stiffened granular pile is evaluated in terms of settlement influence factor, variations of normalized shear stress along GP-soil interface and percentage of load transferred to the base.

Parameters affecting the overall response are (i) relative length i.e., length to diameter ratio of the GP, (L/d) , (ii) the relative stiffness of GP, $K_{gp}=(E_{gp}/E_s)$, (iii) the relative stiffness of the bearing stratum, $K_b=E_b/E_s$, in case of the end bearing GP (iv) Poisson's ratios of the soft soil, ν_s and of the bearing stratum, ν_b . (v) Relative length of stiffening from top of GP, $\eta(=L_s/L)$ and (vi) Relative stiffness factor, $\chi = E_{gpst}/E_{gp}$.

The parameter α as defined by Poulos and Mattes (1971) is

$$\alpha = \frac{\text{Additional settlement caused by the adjacent pile}}{\text{settlement of pile under its own load}} \quad (28)$$

For stiffened GP α_{2E} is defined as

$$\alpha_{2E} = \frac{(\text{Settlement of a GP in a group of two partially stiffened GP} - \text{settlement of a single partially stiffened GP})}{\text{settlement of a single partially stiffened GP}} \quad (29)$$

Parameter β_{2E} (settlement reduction factor) is defined as follows,

$$\beta_{2E} = \frac{\text{settlement of GP in a group of two partially stiffened end bearing GP}}{\text{settlement of a GP in a group of two unstiffened end bearing GP}} \quad (30)$$

All the parameters defined above are for partially stiffened GP having relative stiffness factor $\chi > 1$.

5. RESULTS AND DISCUSSION

The results with the present analysis match very closely with differences less than about 1% with those of Poulos and Mattes (1971) for an un-stiffened GP (Table 1).

Table 1 Comparison of values of α for group of two un-stiffened end bearing GPs

PARAMETERS	Group of two un-stiffened end bearing GPs.(Interaction coefficient α)	
	Poulos & Mattes (1971)	Present study
L/d=10, $v_s=0.5$, $v_b=0.5$, s/d=2, $K_{gp}=10$, $E_b/E_s=100$	0.228	0.224
L/d=10, $v_s=0.5$, $v_b=0.5$, s/d=3, $K_{gp}=100$, $E_b/E_s=100$	0.068	0.066
L/d=10, $v_s=0.5$, $v_b=0.5$, s/d=3, $K_{gp}=1000$, $E_b/E_s=100$	0.019	0.018

Results are obtained for the following ranges of non-dimensional parameters: $K_{gp} = 10-1000$, $\eta = 0.1-0.4$, $\chi = 1-12$, $v_s = 0.3-0.5$, $v_b = 0.3-0.5$, $L/d = 10-40$, $s/d = 2-8$, $E_b/E_s = 10-1000$. Poisson's ratios of surrounding soil and base stratum do not affect the results significantly. Although the realistic normal range of K_{gp} , is 10-100, the study has been carried out for K_{gp} of range 10- 1000.

Figure 3 presents the variations of top settlement influence factor with the relative stiffness of GP for $L/d=10$, relative stiffness of bearing stratum, $E_b/E_s = 100$, relative length of stiffening from top of GP, $\eta = 0.2$ and for both single and two groups of GP at spacing, $s/d=2$. For an un-stiffened single GP, i.e., $\chi = 1$, the factor decreases from about 0.27 at $K_{gp} = 10$, to 0.014 at K_{gp} , equal to 1000. The top settlement influence factor decreases with increasing stiffening quantified by the relative stiffness parameter, χ . This effect decreases with increasing relative stiffness, K_{gp} , of GP. The top settlement influence factor for single GP decreases from about 0.27 for homogeneous GP ($\chi=1$) at $K_{gp}=10$ to about 0.204 and 0.184 for χ equal to 4 and 12 respectively, reductions of the order of 24.4 and 31.8 percent respectively. For $K_{gp}=100$, in case of single GP, top settlement influence factor decreases from about 0.077 for un-stiffened GP ($\chi=1$) to about 0.064 and 0.061 for χ equal to 4 and 12 respectively, reductions of about 16.8 and 20.7 percent respectively. But for a relatively very stiff single GP with $K_{gp}=1000$, settlement influence factor decreases marginally from about 0.014 for un-stiffened GP ($\chi=1$) to about 0.013 and 0.012 for χ equal to 4 and 12 respectively, reductions of about 7 and 14 percent respectively,

attesting to the beneficial effect of stiffening of GP for relatively less stiff GP, i.e., K_{gp} in the range 10 to 100.

The variations of settlement influence factor of GP in group of two with K_{gp} , follow the same trends as those for single GP but with larger magnitudes as expected (Poulos and Davis 1980) as shown in Figure 3. The top settlement influence factor for GP in two pile group for $\chi=1, 4$ and 12 are 0.336, 0.264, and 0.244 respectively for $K_{gp}=10$. The percentage increases with respect to single pile at $K_{gp}=10$, are of the order of 24, 29 and 32 respectively and nearly the same for all degrees of stiffening. This increase is quantified in terms of the interaction factor, α_{2E} , defined as (I_{sp} for pile in two pile group - I_{sp} for single GP) / I_{sp} for single GP. The variations of α_{2E} , with K_{gp} , for different relative stiffness parameters, χ and relative stiffness of bearing stratum, E_b/E_s , are presented in Figure 8.

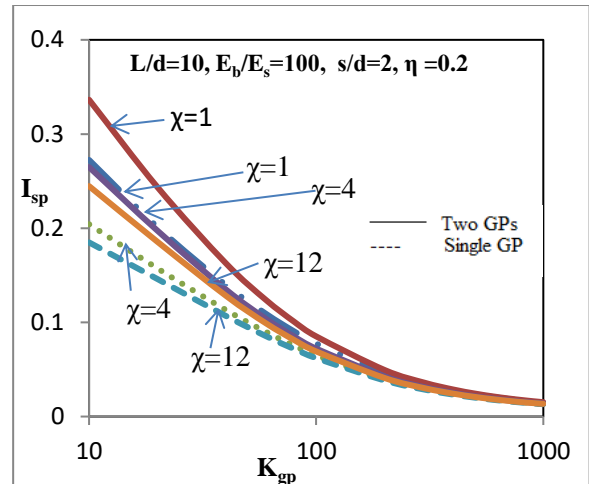


Figure 3 Variation of top settlement influence factor, I_{sp} , with relative stiffness of GP, K_{gp} —Effect of relative stiffness factor, χ , on a GP for single and group of two partially stiffened end bearing GPs ($L/d=10$, $E_b/E_s=100$, $s/d=2$, $\eta=0.2$)

The variation of top settlement influence factor, I_{sp} , with relative length of stiffening from top of GP, η , with the effect of relative stiffness factor, χ , for $L/d=10$, $s/d=2$, $K_{gp}=50$ and $E_b/E_s=100$, reveals that for a single un-stiffened GP, i.e., $\chi=1$, I_{sp} , is about 0.122 while the corresponding values for $\chi=4$ and $\eta=0.1, 0.2, 0.3$ and 0.4 are respectively 0.110, 0.100, 0.091 and 0.084, the percentage decreases of about 9, 18, 25 and 31 (Figure 4).

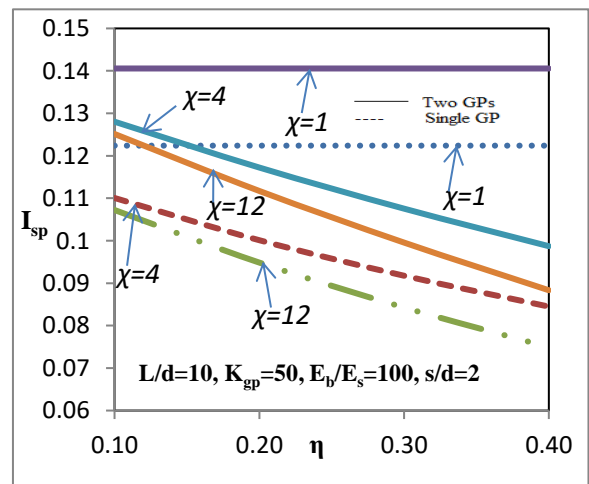


Figure 4 Variation of top settlement influence factor, I_{sp} , with relative length of stiffening from top of GP, η —effect of relative stiffness factor, χ , on a GP for single and group of two partially stiffened end bearing GPs ($L/d=10$, $K_{gp}=50$, $E_b/E_s=100$, $s/d=2$)

The effect is not so significant for χ in the range 4 to 12. The same trend of variation of top settlement influence factor of GP in a group of two with, K_{gp} , is followed as that for a single GP but with larger magnitudes (Figure 4). I_{sp} , for a group of two un-stiffened GPs is about 0.141 with $L/d=10$, $K_{gp}=50$, $E_b/E_s=100$, $s/d=2$ while the corresponding values for $\chi=4$, and $\eta=0.1, 0.2, 0.3$ and 0.4 are respectively 0.128, 0.117, 0.107 and 0.098 with percentage decreases of about 9, 17, 24 and 30.

It can be seen (Figure 5) that top settlement influence factor, I_{sp} , is more for group of two partially stiffened end bearing GPs because of the influence of one pile over the other. For single GP with $L/d=10$, $K_{gp}=50$, $E_b/E_s=100$, $\eta=0.3$ and $\chi=1, 2, 4$ and 8 , the values of I_{sp} , are 0.122, 0.102, 0.091 and 0.08 respectively, with percentage decreases of 16, 25 and 34 respectively with χ . For group of two GPs with the same set of parameters but with $s/d=2$, the values of I_{sp} , are 0.14, 0.119, 0.107 and 0.101 respectively percentage decreases of 15, 23.5 and 28 respectively. The percentage reduction in top settlement is less with lower value of relative length of stiffening from top of GP, η . Considerable reduction in top settlement occurs mainly in the range of $\chi=1-3$.

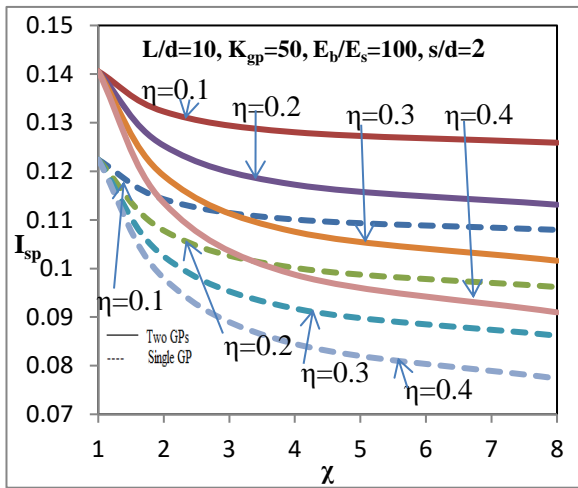


Figure 5 Variation of top settlement influence factor, I_{sp} , with relative stiffness factor, χ —effect of relative length of stiffening from top of GP, η , on a GP for single and group of two partially stiffened end bearing GPs ($L/d=10$, $K_{gp}=50$, $E_b/E_s=100$, $s/d=2$)

Figure 6 represents the variation of settlement influence factor, I_{spd} , of GP in a group of two GPs with normalized depth, $z^*=z/L$ for un-stiffened and stiffened conditions for $s/d=3$, $\eta=0.3$, $L/d=10$, $K_{gp}=100$ and $E_b/E_s=100$. The variation is smooth and continuous without any kink attesting that the compatibility of displacements at the interface of stiffened and un-stiffened portions of the GP is satisfied. The settlement influence factors, I_{spd} , are respectively 0.082, 0.070, 0.066 and 0.0644 for $\chi=1$ (un-stiffened), and 2, 3 and 4 (stiffened). Percentage decreases of settlement are about 14, 19 and 22 respectively due to the effect of stiffening. Percentage decrease of settlement is large for χ increasing from 1 to 2, as compared to those with further increases in χ . The stiffening effect on settlement influence factor is negligible for $z^* > 0.3$ for all values of χ .

The settlement influence factors, I_{spd} , are respectively 0.080, 0.075, 0.072 and 0.069 (Figure 7) for relative length of stiffening of GP, η , equal to 0.1, 0.2, 0.3 and 0.4 for $\chi=2$, $L/d=10$, $K_{gp}=100$, $s/d=2$ & $E_b/E_s=100$. Fig. 8 depicts the variation of settlement interaction factor, α_{2E} , with relative stiffness of GP, K_{gp} , with the effect of relative stiffness factor, χ and relative stiffness of bearing stratum, E_b/E_s , for $L/d=10$, $s/d=3$ and $\eta=0.3$. The effect of relative stiffness of GP, K_{gp} , on decrement in settlement interaction factor, α_{2E} , is significant for K_{gp} in the range 10-100. The value of α_{2E} , for $K_{gp}=10$ and $E_b/E_s=100$ is 0.15 for $\chi=1$ (un-stiffened condition). Corresponding values of α_{2E} are 0.19 and 0.21 for $\chi=4$ & 12 i.e., percentage increase, of 26 and 40

respectively. The value of α_{2E} , for $K_{gp}=10$ is (Figure 8) 0.159 for $E_b/E_s=10$ for un-stiffened GP and increases to 0.20 and 0.25 for, $\chi=4$ & 12 respectively, percentage increase of 25 and 57 respectively. At higher values of K_{gp} (> 200) the values of α_{2E} , converge to a single value.

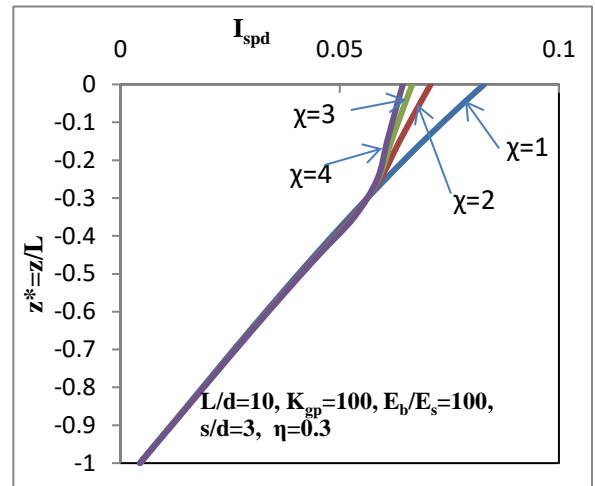


Figure 6 Variation of settlement influence factor for any depth, I_{spd} , with normalized depth, $z^*=z/L$ —effect of relative stiffness factor, χ , for a group of two partially stiffened end bearing GPs ($L/d=10$, $K_{gp}=100$, $E_b/E_s=100$, $s/d=3$, $\eta=0.3$)

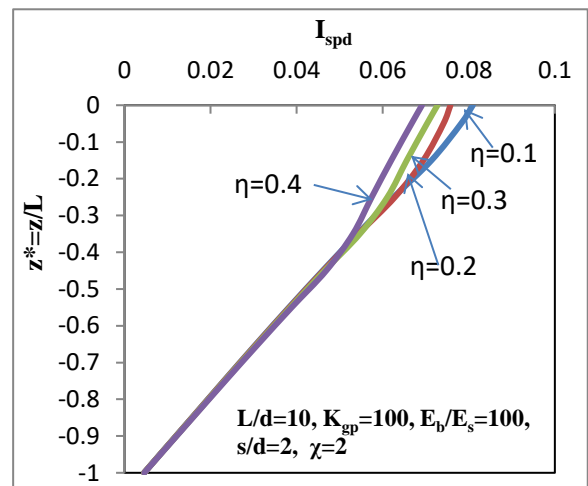


Figure 7 Variation of settlement influence factor for any depth, I_{spd} , with normalized depth, $z^*=z/L$ —effect of relative length of stiffening from top of GP, η , for a group of two partially stiffened end bearing GPs ($L/d=10$, $K_{gp}=100$, $E_b/E_s=100$, $s/d=2$, $\chi=2$)

The effect of stiffening of GPs is better quantified in terms settlement reduction factor, β_{2E} , (ratio of stiffened to un-stiffened factors for GPs). Figure 9 shows linear variation of β_{2E} with relative length, η , of stiffening from top of GP, for relative stiffness factors, χ , equal to 2, 4 and 12 and K_{gp} equal to 50 and 100. The values of β_{2E} , for $K_{gp}=100$ are 0.94, 0.92 and 0.89 for $\chi=2, 4, 12$ respectively for $L/d=10$, $s/d=3$, $E_b/E_s=100$ $\eta=0.1$ corresponding to percentage decreases in β_{2E} of 2 and 5 respectively with respect to $\chi=2$. Similarly, for $\chi=2$, $K_{gp}=50$ the values of β_{2E} are 0.94, 0.90, 0.85 and 0.81 for $\eta=0.1, 0.2, 0.3$ and 0.4 respectively, with percentage decreases of 4, 9 and 14.

Figure 10 shows the variation of settlement reduction factor, β_{2E} , with relative stiffness factor, χ , for two values (50 and 100) of relative stiffness of GP, K_{gp} . For un-stiffened GP with, $\chi=1$ the value of, β_{2E} , is 1 and it can be seen from the graph that for $L/d=10$, $K_{gp}=100$, $s/d=2$, $\eta=0.2$ and $E_b/E_s=100$, the values of β_{2E} , decrease from 1 to 0.9,

0.86 and 0.84 for $\chi = 1, 2, 3$ and 4 respectively. Percentage decreases in value of, β_{2E} , are about 10, 14 and 16 and confirm that stiffening is mainly effective for χ in range of 1-3. It can also be observed from Fig.10 that with increase in relative length, L/d , the values of settlement reduction factor, β_{2E} , decrease, e.g., for $K_{gp}=100$, $s/d=2$, $\eta=0.2$ and $E_b/E_s=100$ the values of β_{2E} , for $\chi=2$, are 0.90, 0.88 and 0.84 for $L/d=10, 20$ and 40 respectively.

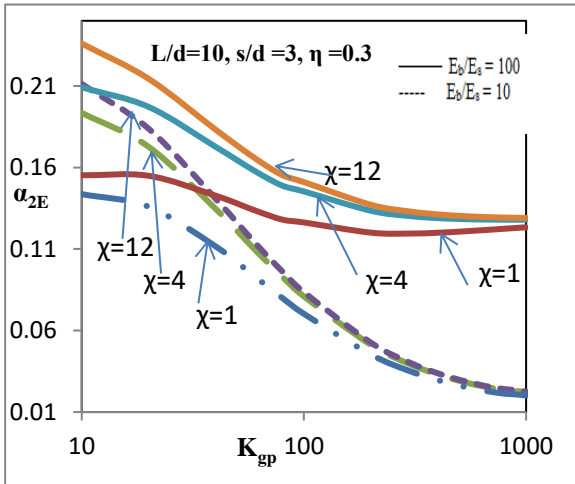


Figure 8 Variation of settlement interaction factor, α_{2E} , with relative stiffness of GP, K_{gp} —effect of relative stiffness factor, χ and relative stiffness of bearing stratum, E_b/E_s , for a group of two partially stiffened end bearing GPs ($L/d=10$, $s/d=3$, $\eta=0.3$)

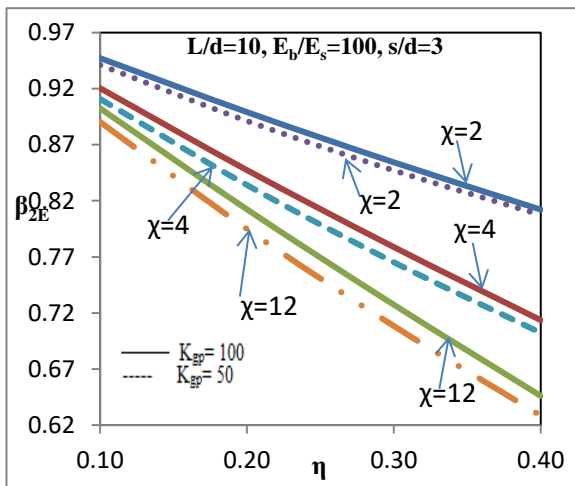


Figure 9 Variation of settlement reduction factor, β_{2E} , with relative length of stiffening from top of GP, η —effect of relative stiffness factor, χ and relative stiffness of GP, K_{gp} , for a group of two partially stiffened end bearing GPs ($L/d=10$, $E_b/E_s=100$, $s/d=3$)

Percentage load transferred to the base, $(P_b/P)_{2EX100}$, is insensitive to relative stiffness factor, χ , for different relative lengths of stiffening from top of GP, η and relative stiffness of GP, K_{gp} , in a group of two partially stiffened end bearing GPs (Figure 11) for $L/d=10$, $E_b/E_s=100$ and $s/d=2$.

Figure 12 also confirms that the percentage load transferred to the base, $(P_b/P)_{2EX100}$, is nearly constant with relative stiffness factor, χ , for all relative stiffness of bearing stratum, E_b/E_s and relative stiffness, K_{gp} , of GP, in a group of two partially stiffened end

bearing GPs for $L/d=10$, $s/d=2$ and $\eta=0.2$ but depends on $E_b/E_s=10, 50$ and 1000 with the values of $(P_b/P)_{2EX100}$, being respectively 64.5, 75.4 and 79.2.

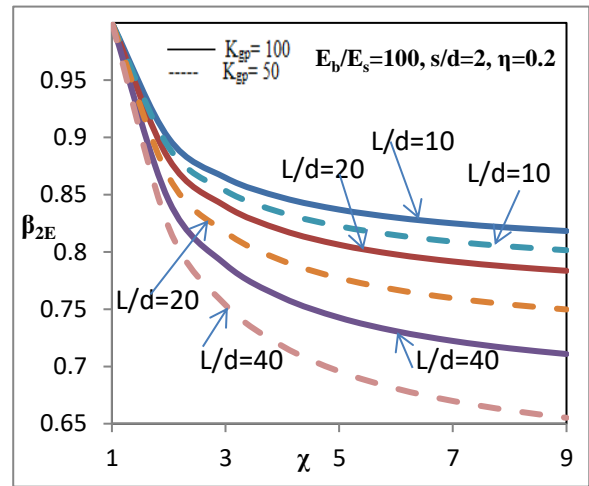


Figure 10 Variation of settlement reduction factor, β_{2E} , with relative stiffness factor, χ —effect of relative length, L/d and relative stiffness of GP, K_{gp} , for a group of two partially stiffened end bearing GPs ($E_b/E_s=100$, $s/d=2$, $\eta=0.2$)

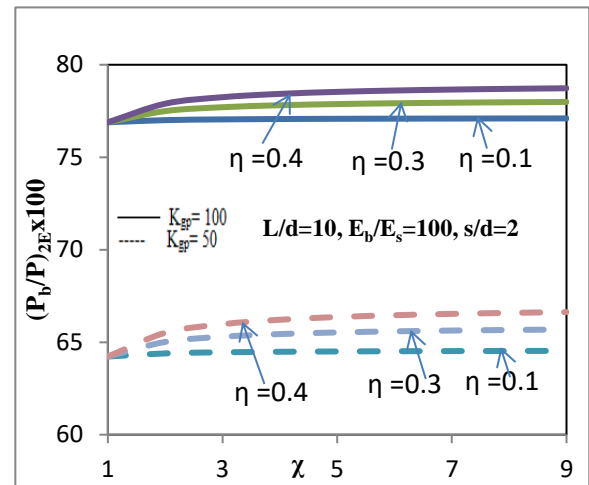


Figure 11 Variation of percentage load transferred to the base, $(P_b/P)_{2EX100}$, with relative stiffness factor, χ —effect of relative length of stiffening from top of GP, η and relative stiffness of GP, K_{gp} , on a GP in a group of two partially stiffened end bearing GPs ($L/d=10$, $E_b/E_s=100$, $s/d=2$)

Figure 13(a) represents the variation of normalized shear stresses, $\tau^*_{2E} = \tau(\pi dL)/P$, with the normalized depth, $z^*=z/L$ for different relative stiffness factors, χ , $L/d=10$, $K_{gp}=100$, $E_b/E_s=100$, $s/d=3$ and $\eta=0.3$. With increase in relative stiffness factor, χ , from 1 to 5 the shear stress at the top of the GP reduces from 0.98 for un-stiffened GP i.e., $\chi=1$ to 0.72 ($\chi=2$), 0.63 ($\chi=3$), 0.55 ($\chi=5$). The shear stresses at the bottom are negative as reported by Poulos (1971). Figure 13(b) represents the variation of normalized shear stresses, $\tau^*_{2E} = \tau(\pi dL)/P$, with the normalized depth, $z^*=z/L$ for different relative lengths of stiffening, η , on a GP for $L/d=10$, $K_{gp}=100$, $E_b/E_s=100$, $s/d=3$ and $\chi=2$. For $\eta=0.1, 0.2, 0.3$ and 0.4 the shear stresses at the top are respectively 0.81, 0.70, 0.67 and 0.64, corresponding to percentage reductions in stresses at the top by respectively 13, 17 and 21.

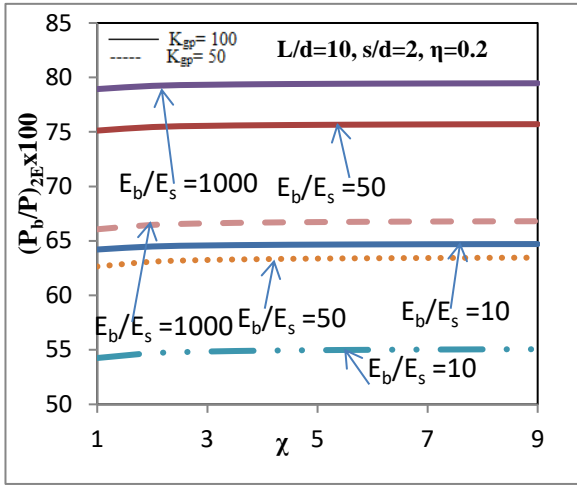


Figure 12 Variation of percentage load transferred to the base, $(P_b/P)_{2E} \times 100$, with relative stiffness factor, χ – effect of relative stiffness of bearing stratum, E_b/E_s and relative stiffness of GP, K_{gp} on a GP in a group of two partially stiffened end bearing GPs ($L/d=10, s/d=2, \eta=0.2$)

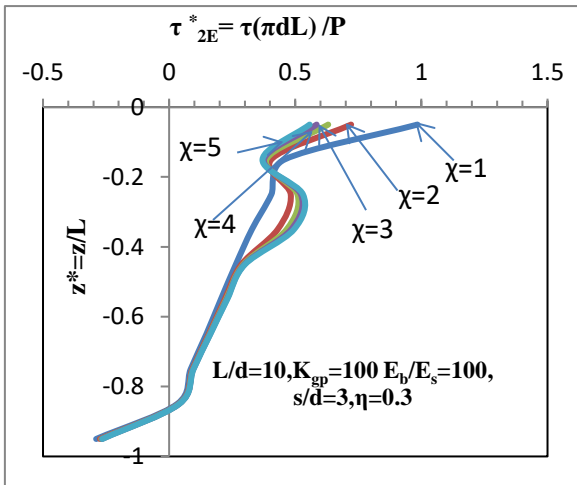


Figure 13(a) Variation of normalized shear stresses, $\tau^*_{2E} = \tau(\pi dL)/P$, with the normalized depth, $z^* = z/L$ – effect of relative stiffness factor, χ , on a GP in a group of two partially stiffened end bearing GPs ($L/d=10, K_{gp}=100, E_b/E_s=100, s/d=3, \eta=0.3$)

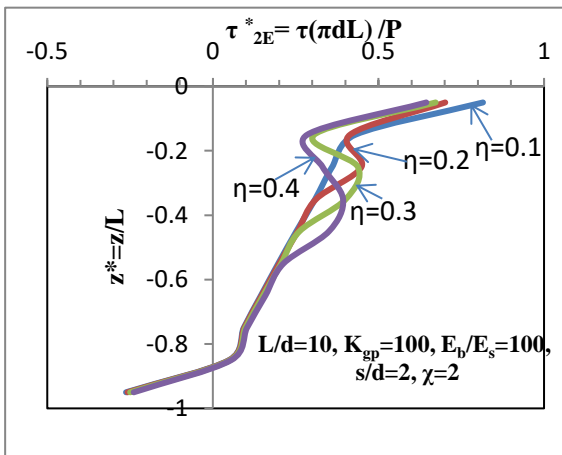


Figure 13(b) Variation of normalized shear stresses, $\tau^*_{2E} = \tau(\pi dL)/P$, with the normalized depth, $z^* = z/L$ – effect of relative length of stiffening from top of GP, η , on a GP in a group of two partially stiffened end bearing GPs ($L/d=10, K_{gp}=100, E_b/E_s=100, s/d=2, \chi=2$)

6. CONCLUSIONS

Partially stiffened single and group of two GP bearing on a stiff stratum have been analysed based on the elastic continuum approach and Mindlin's equations. A new pile displacement matrix is developed incorporating the stiffening parameters viz. relative stiffness factor, χ , and relative length of stiffening from top, η .

1. Top settlement influence factor, I_{sp} , for single and group of two partially stiffened end bearing GPs reduces with increasing relative stiffness factor, χ . For single partially stiffened pile percentage reduction is about 23% for relative stiffness factor, χ , increasing from 1 to 8 for $K_{gp} = 100, L/d=10, E_b/E_s=100, s/d=2$, and relative length of stiffening from top, $\eta = 0.2$.
2. For a group of two partially stiffened end bearing GPs, top settlement influence factor, I_{sp} , reduces by about 18% for χ increasing from 1-8 for $K_{gp} = 100, L/d=10, E_b/E_s=100, s/d=2$, and relative length of stiffening from top of GP, $\eta = 0.2$.
3. The settlement reduction factor, β_{2E} , reduces with increasing stiffening parameters, χ and η . Reduction is about 23% with relative stiffness factor, χ , increasing from 1 to 3 for $K_{gp} = 100, L/d=10, E_b/E_s=100, s/d=3, \eta = 0.3$ and by about 27% for relative stiffness factor, χ , increasing from 1 to 8. Stiffening is significant in the range of stiffness factor increasing from 1 to 3.
4. Settlement reduction factor, β_{2E} , increases with increase in relative stiffness of bearing stratum (E_b/E_s), relative stiffness of granular pile (K_{gp}), normalized spacing (s/d). Settlement reduction factor, β_{2E} , reduces by 12% for relative length of stiffening from top, η , increasing from 0.1 to 0.4 for $K_{gp} = 100, L/d=20, E_b/E_s=100, s/d=2$ and $\chi=2$.
5. Percentage load transferred to the base increases marginally with increase in stiffening parameters.
6. Normalized shear stresses in case of group of two partially stiffened GPs reduce by about 42% at the top of the GP, due to stiffening for the relative stiffness factor, χ , increasing from 1 to 5 for $\eta=0.3, K_{gp}=100, L/d=10, E_b/E_s=100$ and $s/d=3$.
7. Settlement interaction factor, α_{2E} , increases 18% for the relative stiffness factor, χ , increasing from 1 to 8 for $K_{gp} = 100, L/d=10, E_b/E_s=100, s/d=3$ and $\eta = 0.3$. Settlement interaction factor, α_{2E} , increases with relative length of stiffening, η , and relative length, L/d , and decreases with relative stiffness of bearing stratum, E_b/E_s , and normalized spacing, s/d .
8. Present study gives the numerical approach to show the effect of partial stiffening of GP. Design charts are ready including the various normalized geometric and strength parameters to study the effect for wide variations. Designers can use these charts by selecting the parameters like relative stiffness factor, relative length of stiffening along with relative length of GP and relative stiffness of bearing stratum with suitable normalized spacing.

7. ABBREVIATIONS

GP	Granular pile
L	Length of granular pile
n	Total number of elements of GP
d	Diameter of granular pile
L/d	Relative length of GP
P	Load on each granular pile
P_b	Load on the base of the GP
E_{gp}	Deformation modulus of un-stiffened portion of granular pile
E_s	Deformation modulus of soil

E_{gpst}	Deformation modulus of stiffened portion of granular pile
E_b	Deformation modulus of bearing stratum
ν_b	Poisson's Ratio of bearing stratum
ν_s	Poisson's Ratio of soil
K_{gp} $= (E_{gp}/E_s)$	Relative stiffness of granular pile
p_b	Pile base pressure
z	Depth of granular pile section taken from the top of granular pile
$z^* (= z/L)$	Normalized depth of GP
s	Spacing between center to center of the piles
s/d	Normalized spacing center to center between piles
I_{sp}	Top settlement influence factor
τ	Shear stress
$\tau_{2E}^* = \tau(\pi dL)/P$	Normalized shear stresses of a GP in group of two GPs
L_s	Length of the pile stiffened from the top of the pile
$\eta = L_s/L$	Relative length of stiffening from top of GP
$\chi = E_{gpst}/E_{gp}$	Relative stiffness factor
ρ	Normalized displacement of GP along its length
$S_{any\ depth}$	Settlement at any depth of GP
S_{TOP}	Settlement at top of the GP
α_{2E}	Settlement interaction factor in group of two GPs
β_{2E}	Settlement reduction factor in group of two GPs
$(P_b/P)_{2EX100}$	Percentage load transferred to the base of a GP in group of two GPs
I_{spd}	Settlement influence factor for any depth
E_b/E_s	Relative stiffness of bearing stratum

8. REFERENCES

Ayadat, T. and Hanna, A.M. (2005), Encapsulated stone columns as a soil improvement technique for collapsible soil, *Ground Improvement*, 9 (4), 137–147.

Black, J.A., Sivakumar, V., Madhav, M.R. and Hamill, G.A. (2007), Reinforced stone columns in weak deposits: laboratory model study, *J of Geotechnical and Geoenvironmental Engineering*, 133 (9), 1154–1161.

Castro, J. and Sagaseta, C. (2011), Deformation and consolidation around encased stone columns, *Geotextiles and Geomembranes*, 29, 268–276.

Garg, V. and Sharma, J.K. (2018), Analysis and settlement of partially stiffened single and group of two floating granular piles, *Indian Geotechnical Journal*, Doi-10.1007/s40098-018-0321-7.

Hong, Y.S., Wu, C.S. and Yu, Y.S. (2016), Model tests on geotextile-encased granular columns under 1-g and un-drained conditions, *Geotextiles and Geomembranes*, 44 (1), 13–27.

Jamsawang, P., Bergado, D.T., Bandari, A. and Voottipruex, P. (2008), Investigation and simulation of behavior of stiffened deep cement mixing (SDCM) piles, *International Journal of Geotechnical. Engg.*, 2(3), 229–246.

Lo, S. R., Zhang, R. and Mak, J. (2010), Geosynthetic-encased stone columns in soft clay: a numerical study, *Geotextiles and Geomembranes*, 28, 292–302.

Madhav, M.R., Sharma, J.K. and Chandra, S. (2006), Analysis and settlement of a non-homogeneous granular pile, *Indian Geotechnical Journal*, 36(3), 249-271.

Marto, A., Moradi, R., Helmi, F., Latifi N. and Oghabi, M. (2013), Performance Analysis of Reinforced Stone Columns using Finite Element Method, *Electronic J of Geotechnical Engineering*, 18, 315-323.

Mattes, N. S. and Poulos, H. G. (1969), Settlement of single compressible pile, *J of SM and F Div., ASCE*, 95, SM1, 189-207.

Mindlin, R.D. (1936), Force at a point in the interior of a semi infinite solid, *Physics*, 7, 195-202.

Murugesan, S. and Rajagopal, K. (2006), Geosynthetic encased stone columns: Numerical evaluation, *Geotextiles and Geomembranes*, 24, 349–358.

Murugesan, S. and Rajagopal, K. (2010), Studies on the behavior of single and group of geosynthetic encased stone columns, *Journal of Geotechnical and Geoenvironmental Engineering*, 136(1), 129–139.

Niroumand, H., Kassim, K.A., and Yah, C.S. (2011), Soil improvement by reinforced stone columns based on experimental work, *The Electronic Journal of Geotechnical Engineering*, 16(7), 1477–99.

Poulos, H. G. and Mattes, N. S. (1971), Settlement and load distribution analysis of pile groups, *Aust. Geomech. J.*, G2(1), 11-20.

Poulos, H.G. and Davis, E.H. (1980), *Pile Foundation Analysis and Design*, John Wiley & Sons Australia.

Pulko, B., Majes, B. and Logar, J. (2011), Geosynthetic-encased stone columns: analytical calculation model, *Geotextiles and Geomembranes*, 29, 29–39.

Shahu, J.T. and Reddy, Y. R. (2011), Clayey soil reinforced with stone column group: model tests and analyses, *Journal of Geotechnical and Geoenvironmental Engineering*, 137 (12), 1265–1274.

Sharma, J. K. (1999), Analysis and settlement of granular pile(s) - single, in group and with raft, A thesis submitted for the degree of Doctor of Philosophy to the Department of Civil Engineering, Indian Institute of Technology, Kanpur, India.

Sharma, R.S., Phani Kumar, B.R., and Nagendra, G. (2004). Compressive load response of stone piles reinforced with geogrids, *Canadian geotechnical journal*, 41, 187–192.

Zhang, L. and Zhao, M. (2015), Deformation analysis of geo-textile encased stone columns, *Int. J of Geomechanics*, 15 (3), 1-10.